

The prompt-early afterglow connection in GRBs

ROBERT MOCHKOVITCH
FRÉDÉRIC DAIGNE*Institut d'Astrophysique de Paris, 98Bis Bd Arago, 75014 Paris, France*

ROMAIN HASCOËT

*Physics Department and Columbia Astrophysics Laboratory, Columbia University,
538 West 120th Street New York, NY 10027*

We study the observed correlations between the duration and luminosity of the early afterglow plateau and the isotropic gamma-ray energy release during the prompt phase. We discuss these correlations in the context of two scenarios for the origin of the plateaus. In the first one the afterglow is made by the forward shock and the plateau results from variations of the microphysics parameters while in the second one the early afterglow is made by a long-lived reverse shock propagating in a low Γ tail of the ejecta.

PRESENTED AT

“Huntsville in Nashville” Gamma-Ray Burst Symposium
Nashville, USA, April 14–18, 2013

1 Introduction

Before the launch of the *Swift* satellite in 2004 [1], the afterglow was believed to be the best understood part of the GRB phenomenon, being explained by the energy dissipated in the forward shock formed by the jet impacting the burst environment. However, the many surprises of the early X-ray afterglow revealed by *Swift* – initial steep decay, plateau phase, flares [2] – have considerably complicated the picture. Several mechanisms have been proposed to explain the plateau but none appears fully convincing.

The recent discovery of correlations linking prompt and early afterglow quantities [3, 4] such as $E_{\gamma,\text{iso}}$, t_p , the duration of the plateau and L_p , the plateau luminosity, represents new constraints to be satisfied by models. After a critical discussion of the case where the plateau is made by late energy injection into the forward shock we consider two alternative scenarios and check if they can agree with the observed correlations.

2 Making a plateau with late energy injection

Continuous energy injection into the forward shock remains a commonly invoked cause of plateau formation. For the most extended plateaus it however imposes to inject several hundreds times more energy than was initially present to power the prompt phase. This huge amount of energy leads to an “efficiency crisis” for the prompt mechanism, whatever it is. Let E_0 and $E = k E_0$ be respectively the values of the energy available during the prompt phase and after injection. Then, the measured gamma-ray efficiency is

$$f_{\gamma,\text{mes}} = \frac{E_{\gamma}}{E_{\gamma} + E} \quad (1)$$

because the energy in the forward shock is estimated from multiwavelength fits of the afterglow after typically one day (i.e. after energy injection). However the true efficiency

$$f_{\gamma,\text{true}} = \frac{E_{\gamma}}{E_{\gamma} + E_0} = \frac{1}{1 + \frac{1}{k} \left(\frac{1}{f_{\gamma,\text{mes}}} - 1 \right)} \quad (2)$$

can be much larger. With for example $f_{\gamma,\text{mes}} = 0.1$, the true efficiency is $f_{\gamma,\text{true}} = 0.53$ for $k = 10$ and 0.92 for $k = 100$. These values of $f_{\gamma,\text{true}}$ seem unreachable for any of the proposed prompt mechanisms: the efficiency of internal shocks can barely reach 10% while that of comptonized photosphere or reconnection models is more uncertain but probably does not exceed 30%.

3 Making a plateau without energy injection

3.1 Within the standard forward shock scenario

Without energy injection the standard forward shock scenario can successfully account for the afterglow evolution after about one day but fails to reproduce the plateau phase. A backwards extrapolation of the late afterglow flux lies above the plateau, which might therefore be interpreted as the indication that some radiation is “missing”. This can be the case if the radiative efficiency of the forward shock during the early afterglow is smaller than predicted by the standard model. The most obvious way to reduce the efficiency is to relax the assumption that the microphysics parameters stay constant throughout the whole afterglow evolution [5, 6]. For both a uniform and a wind external medium the afterglow X-ray flux behaves as

$$F_X \propto E^{\frac{p+2}{4}} \epsilon_e^{p-1} \epsilon_B^{\frac{p-2}{4}} t^{-\frac{3p-2}{4}} \quad (3)$$

where E is the burst isotropic energy, ϵ_e and ϵ_B the microphysics parameters and p the power-law index of the accelerated electron spectrum. With $2 < p < 3$ the dependence on ϵ_B is weak so that in practice only playing with ϵ_e can really affect the flux evolution. A priori ϵ_e can be a function of the shock Lorentz factor, the density of the external medium (if it is a stellar wind) or both.

The stellar wind case is especially interesting if one assumes that, below a critical density n_0 , ϵ_e is constant while $\epsilon_e \propto n^{-\nu}$ (with $\nu > 0$) for $n > n_0$. Since the density seen by the forward shock is given by $n(t) \sim 6.3 \cdot 10^4 A_*^2 E_{53}^{-1} t^{-1} \text{ cm}^{-3}$ (where A_* is the wind parameter; see [7]) the transition at n_0 , which corresponds to the end of the plateau, takes place at

$$t_p \approx 6.6 \cdot 10^4 A_*^2 n_0^{-1} E_{53}^{-1} \approx 6.6 \cdot 10^4 A_*^2 n_0^{-1} f_\gamma E_{\gamma,53}^{-1} \text{ s} \quad (4)$$

where f_γ is the gamma-ray efficiency of the prompt phase and $E_{\gamma,53}$ is the isotropic gamma-ray energy release. If the product $A_*^2 n_0^{-1} f_\gamma$ does not vary much from burst to burst (and stays close to about 0.1) Eq.(4) is not too different from the observed $[t_p, E_{\gamma,\text{iso}}]$ relation.

A flat plateau is obtained for $\nu = \frac{3p-2}{4(p-1)} = \nu_0 = 0.92$ if $p = 2.5$ while for $\nu < \nu_0$ (resp. $\nu > \nu_0$) the plateau flux is decreasing (resp. rising) with time. Since $n(t) \propto t^{-1}$, a flat plateau extending over two decades in time (as in GRB 060729) requires an increase of ϵ_e by a factor of about 100 from the beginning to the end of the plateau.

3.2 With a long-lived reverse shock

We now suppose that the ejecta emitted by the central engine is made of a “head” with material at high Lorentz factors ($\Gamma \sim 10^2 - 10^3$), followed by a “tail” where the

Lorentz factor decreases to much smaller values, possibly close to unity. The head is responsible for the prompt emission while the reverse shock propagating through the tail makes the afterglow [8, 9].

We adopt for the head a constant energy injection rate \dot{E}_H for a duration of 10 s. We do not specify the distribution of the Lorentz factor and simply consider its average value, supposed to be $\bar{\Gamma} = 400$. The tail that follows lasts for 100 s but this value is not critical as long as it does not exceed the duration of the early steep decay phase observed at the beginning of most X-ray light curves. We start with a simple case where the distribution of energy in the tail $\frac{dE}{d\text{Log}\Gamma}$ is constant from $\Gamma = 400$ to $\Gamma = 1$. This can be obtained by adopting a constant energy injection rate \dot{E}_T and a Lorentz factor of the form

$$\Gamma_T(s) = 400^{(1.1-s/100)} , \quad (5)$$

from $s = 10$ to 110 light.seconds, the distance s being counted from the front to the back of the flow.

Using the methods described in [8] we have obtained the power $P_{\text{diss}}(t)$ dissipated by the reverse shock (as a function of arrival time to the observer) for $\dot{E}_H = 10\dot{E}_T$ (so that equal amounts of energy are injected in the head and tail, and two possibilities for the burst environment: (i) a uniform medium with $n = 1 \text{ cm}^{-3}$ or (ii) a stellar wind with a wind parameter $A_* = 1$).

Going from the dissipated power to actual light curves depends on assumptions that have to be made for the microphysics parameters but the general shape of the early X-ray afterglow light curves remains globally similar to the evolution of $P_{\text{diss}}(t)$ so that some conclusions can already be reached without having to consider the uncertain post-shock microphysics.

If energy is evenly distributed in the tail (constant $\frac{dE}{d\text{Log}\Gamma}$) a short plateau lasting about 1000s is observed for a uniform external medium while for a stellar wind there is no plateau. In both cases, the dissipated power approximately decays as t^{-1} after about 1000 s. It is larger by a factor 3 - 5 for a uniform medium due to a larger contrast κ of the Lorentz factors at the reverse shock compared to the wind case ($\kappa \simeq 2$ and $2^{1/2}$ respectively, see [8]), leading to a higher efficiency.

We now vary the energy deposition in the tail, concentrating more power at some value of the Lorentz factor. We have for example considered a simple model where

$$\dot{E}_T(\Gamma) = \begin{cases} \dot{E}_* \left(\frac{\Gamma}{\Gamma_*}\right)^{-q} & \text{for } \Gamma > \Gamma_* \\ \dot{E}_* \left(\frac{\Gamma}{\Gamma_*}\right)^{q'} & \text{for } \Gamma < \Gamma_* \end{cases} \quad (6)$$

the value of \dot{E}_* being fixed by the total energy injected in the tail. When energy deposition is more concentrated (increasing q) a plateau progressively forms and becomes flatter. The value of Γ_* in Eq.(6) fixes the duration t_p of the plateau as it approximately corresponds to the time when the reverse shock reaches s_* where $\Gamma_T(s_*) = \Gamma_*$.

The q parameter controls the flatness of the plateau while q' controls the decay index after the plateau. As long as $E_T \lesssim E_H$, the deceleration of the head can be described as if it does not receive any supply of energy from the tail, which gives

$$t_p \sim \begin{cases} 9 \cdot 10^4 E_{H,53}^{1/3} n^{-1/3} \Gamma_{*,1}^{-8/3} \text{ s} & (\text{uniform medium}) \\ 3 \cdot 10^4 E_{H,53} A_*^{-1} \Gamma_{*,1}^{-4} \text{ s} & (\text{stellar wind}) \end{cases} \quad (7)$$

Then, an approximate analytical solution for the power dissipated in the reverse shock can be obtained following the method described in [8]

$$P_{\text{diss}}(t) = \frac{E_T}{t_p \varphi_{qq'}} F(\gamma) \left(\frac{t}{t_p} \right)^{\pm q\gamma - 1}, \quad (8)$$

where $\varphi_{qq'} = \frac{1}{q} + \frac{1}{q'}$ and $F(\gamma) = \frac{\gamma}{2} \left[1 - (1 - 2\gamma)^{1/2} \right]^2$ with $\gamma = 3/8$ (resp. $1/4$) for a uniform medium (resp. a stellar wind). The decay indices before and after the break at the end of the plateau are

$$\begin{aligned} \alpha_1 &= \gamma q - 1 \\ \alpha_2 &= -\gamma q' - 1 \end{aligned} \quad (9)$$

so that a flat plateau is expected for $q = 1/\gamma$ (i.e. $q = 8/3$ and 4 in the uniform medium and wind cases (i) and (ii) respectively). For a typical decay index $\alpha_2 = -1.5$ after the plateau we get the condition $q' = 1/2\gamma$ (i.e. $q' = 4/3$ and 2 for cases (i) and (ii)).

4 Building a sequence of models

4.1 Forward shock scenario

It has been shown in Sect.3.1 that a transition in the behavior of ϵ_e (from rising to constant) at a fixed density n_0 marks the end of the plateau at a time t_p given by Eq.(4). The X-ray luminosity L_p at $t = t_p$ then reads

$$L_p \propto E^{\frac{p+2}{4}} t_p^{-\frac{3p-2}{4}} \propto t_p^{-p} \propto E_{\gamma,\text{iso}}^p \quad (10)$$

as long as the efficiency and the microphysics parameters do not strongly vary from burst to burst. We have obtained a sequence of afterglow light curves for $\epsilon_e = 0.1$, $\epsilon_B = 0.01$, $n_0 = 1.7 \text{ cm}^{-3}$, $f_\gamma = 0.1$, $A_* = 1$ and $p = 2.5$ and different values of the isotropic gamma-ray energy release $E_{\gamma,\text{iso}}$ from which we have plotted the three relations $[L_p, E_{\gamma,\text{iso}}]$, $[L_p, t_p]$ and $[L_p/E_{\gamma,\text{iso}}, t_p]$ shown in Fig.1.

4.2 Reverse shock scenario

Using Eq.(7) it is possible to link the duration of the plateau to the gamma-ray energy release $E_{\gamma,\text{iso}}$, for a given dependence of Γ_* on the burst energy. Adopting $\Gamma_* \propto E^{1/2}$ as suggested in [10] (see however [11]) leads to

$$t_p \propto E^{-1} \propto E_{\gamma,\text{iso}}^{-1} \quad (11)$$

for both a uniform medium and a stellar wind (if the gamma-ray efficiency does not depend on E). Together with Eq.(8) this fixes the dissipated power during the plateau phase

$$P_{\text{diss}} \propto t_p^{-2} \propto E_{\gamma,\text{iso}}^2 \quad (12)$$

To now compute a sequence of X-ray light curves from the dissipated power we need the microphysics parameters ϵ_e and ϵ_B for which we adopt the fiducial values $\epsilon_e = 0.1$ and $\epsilon_B = 0.01$. From this sequence of light curves, we obtain t_p and L_p as a function of $E_{\gamma,\text{iso}}$ and again plot the results in the three diagrams of Fig.1.

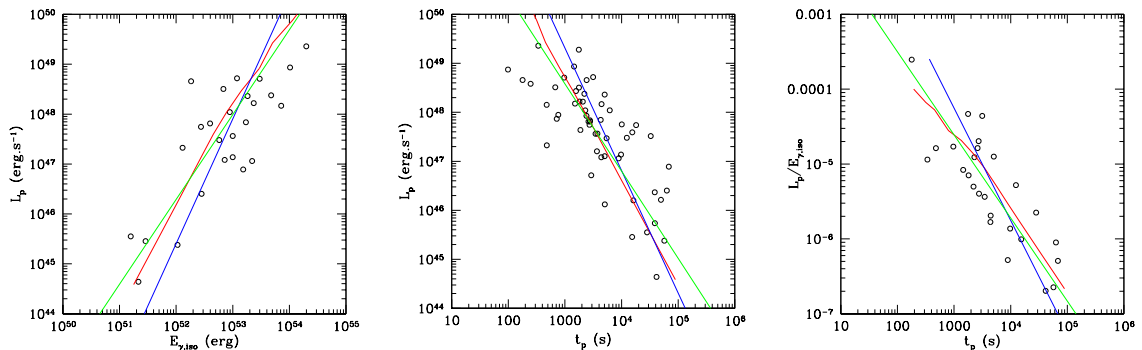


Figure 1: Model $[L_p, E_{\gamma,\text{iso}}]$, $[L_p, t_p]$, and $[L_p/E_{\gamma,\text{iso}}, t_p]$ correlations compared to the data collected by [4]. The green line is the best power-law fit of the data while the blue and red ones respectively correspond to the forward and reverse shock scenarios.

5 Discussion and conclusion

The two scenarios we have considered to account for the origin the X-ray plateau seem able to explain the main features of the prompt-afterglow connection. When compared to data the $[L_p, E_{\gamma,\text{iso}}]$ and $[L_p, t_p]$ correlations however appear somewhat steeper, especially in the forward shock case. The forward shock scenario also imposes a wind external medium and that ϵ_e first increases with decreasing wind density. In the reverse shock case, the shock propagates in a low- Γ tail of the ejecta with a peak of injected power at a Lorentz factor $\Gamma \sim 20 - 30$. This scenario supposes that the

forward shock is (at least initially) radiatively inefficient, as suggested by [12]. It may look more exotic but has an advantage of flexibility as various accidents in the early X-ray afterglow (such as steep breaks, bumps,...) can be simply produced by playing with the distribution of injected power in the tail (see [13]).

ACKNOWLEDGEMENTS

It is a pleasure to thank Raffaella Margutti who kindly sent us her data on the prompt-afterglow correlations. R.H. acknowledges the support by NSF grant AST-1008334.

References

- [1] N. Gehrels, et al., ApJ **611**, 1005 (2004).
- [2] J.A. Nousek et al., ApJ **642**, 389 (2006).
- [3] M.G. Dainotti et al., MNRAS **426**, 218 (2012).
- [4] R. Margutti et al., ApJ **428**, 729 (2013).
- [5] J. Granot, A. Königl & T. Piran, MNRAS **370**, 1946 (2006).
- [6] K. Ioka et al., A&A **458**, 7 (2006).
- [7] A. Panaitescu & P. Kumar, ApJ **543**, 66 (2000).
- [8] F. Genet, F. Daigne & R. Mochkovitch, MNRAS **381**, 732 (2007).
- [9] Z.L. Uhm & A. Beloborodov, ApJ **665**, L93 (2007).
- [10] G. Ghirlanda et al., MNRAS **420**, 483 (2012).
- [11] R. Hascoët et al., arXiv:1304.5813 (2013).
- [12] M. Lemoine & G. Pelletier, MNRAS **418**, L64 (2011).
- [13] Z.L. Uhm et al., ApJ **761**, 147 (2012).